# Multistep Thermosensitivity of Poly(*N*-*n*-propylacrylamide)-*block*-poly(*N*-isopropylacrylamide)-*block*-poly(*N*,*N*-ethylmethylacrylamide) Triblock Terpolymers in Aqueous Solutions As Studied by Static and Dynamic Light Scattering

**Dinghai Xie,[†] Xiaodong Ye,[†] Yanwei Ding,[†] Guangzhao Zhang,[†] Ning Zhao,[‡] Kai Wu,[‡] Ya Cao,[‡,§] and X. X. Zhu*[,‡]**

*Hefei National Laboratory for Physical Sciences at Microscale and Department of Chemical Physics, University of Science and Technology of China, Hefei, Anhui 230026, China, Département de Chimie, Université de Montréal, C.P. 6128, Succursale Centre-ville, Montréal, QC H3C 3J7, Canada, and State Key Laboratory of Polymer Materials Engineering, Sichuan University, Chengdu, Sichuan 610065, China*

*Received December 16, 2008; Revised Manuscript Received March 2, 2009*

ABSTRACT: Poly(*N*-*n*-propylacrylamide)-*block*-poly(*N*-isopropylacrylamide)-*block*-poly(*N*,*N*-ethylmethylacrylamide) (PnPA-*b*-PiPA-*b*-PEMA) triblock terpolymers of low polydispersity have been synthesized by reversible addition-fragmentation chain transfer (RAFT) polymerization via sequential monomer addition. The temperature-induced formation and dissociation of terpolymer micelles in aqueous solutions in a heating−cooling cycle were investigated by a combination of static and dynamic laser light scattering. In the heating process, the folding of PnPA at ca. 25 °C led to the formation of polymeric micelles with a collapsed hydrophobic PnPA core and a hydrophilic swollen PiPA−PEMA shell. Further increase of the temperature to ca. 32 and 53 °C led to the successive dehydration of PiPA and PEMA on the periphery, respectively. Our results revealed that when PEMA on the periphery of the micelle is too short to stabilize the hydrophobic core, individual micelles tend to aggregate into large micellar clusters, corresponding to the intrachain contraction and interchain association of the PiPA chains. In the cooling process, the complete dissolution temperature was lower than the association temperature in the heating process. At a given temperature, the aggregates in the cooling process had a higher mass than those in the heating process, clearly indicating a hysteresis.

## Introduction

Thermosensitive polymers have received much attention because of their potential applications in membranes,[1] drug delivery systems[2] and isolation of biomolecules.[3] The *N*-alkyl substituted polyacrylamides are well-known representatives of the group of thermosensitive polymers with a lower critical solution temperature (LCST) at which a polymer solution undergoes phase transition from a soluble to an insoluble state.[4−13] Recently, block copolymers whose blocks can be reversibly switched from hydrophilic to hydrophobic by a temperature stimulus have been extensively investigated.[14−17] Amphiphilic or double-hydrophilic diblock copolymers comprising a thermosentive block are the most widely studied, which exhibit a single transition.[18−23] More complex and flexible polymers involving multiple transitions are essential in the understanding of the process and in the design and use of interesting molecular device.[15] Doubly thermosensitive diblock copolymers which exhibit two different LCSTs have been investigated by several groups.[24−28] In such systems, a transition from a hydrophilic to an amphiphilic and finally to a hydrophobic block copolymer occurs with an increase in temperature.[24,25,27] Some of the doubly thermosensitive diblock copolymers even present an interesting self-association behavior, which undergo multiple transitions upon heating.[26,28] Thermosensitive triblock copolymers have attracted considerable interest because of their complex morphologies.[29−39] To date, most reports are focused on ABA or BAB triblock copolymers with A representing the hydrophilic block and B the thermosensitive block. The self-assembly behavior of ABA triblock copolymers is very similar to that of the AB diblock copolymers,[38] while a BAB architecture tends to yield more complex structure such as flower-like or interconnected micelles and networks.[32−35,39] The above-mentioned AB, ABA, and BAB block copolymers represent all-or-none systems with respect to temperature-responsive amphiphilicity and associative behavior in aqueous solutions. Under many circumstances, more gradual or more subtle thermosensitivity are desirable. This may be realized by the use of thermosensitive ABC triblock copolymers in which a hydrophilic block is combined with two different thermosensitive blocks.[31,33,37] Two evident thermal transitions are observed in dilute aqueous solutions of such double thermosensitive ABC triblock copolymers.[31,33] In addition to block copolymers, doubly thermosensitive unimolecular micelles have been reported and two-stage collapse processes were observed.[40] Recently, we have synthesized well-defined ABC triblock copolymers by reversible addition-fragmentation chain transfer (RAFT) polymerization via sequential monomer addition.[41−43] Our ternary block copolymers consist of three different thermosensitive blocks with different cloud points (CP), exhibiting more complex and interesting aggregation behaviors in water. Such polymers exhibited multiple thermosensitivity with accompanying changes in micellar size or shape and solution properties.[43] The aggregation mechanism of such multiblock copolymers remains to be explored, and the effect of the length of the final block of the copolymers on their aggregation in solution needs to be elucidated. We use a combination of static and dynamic light scattering (LS), and

* To whom correspondence should be addressed. E-mail: julian.zhu@umontreal.ca.
[†] Hefei National Laboratory for Physical Sciences at Microscale and Department of Chemical Physics, University of Science and Technology of China.
[‡] Département de Chimie, Université de Montréal.
[§] State Key Laboratory of Polymer Materials Engineering, Sichuan University.

10.1021/ma802801h CCC: $40.75 
Published on Web 03/17/2009

the ultrasensitive differential scanning calorimetry (US-DSC) to study the micellization of the PnPA-*b*-PiPA-*b*-PEMA triblock copolymers with identical PnPA and PiPA blocks but a PEMA block of different lengths. Our results confirm that the length of third PEMA block plays a key role in the formation of micellar clusters. When the PEMA block is long enough, no micellar clusters are formed. A two-stage hydration process of the PnPA and PiPA blocks is observed for the first time in the cooling process during the US-DSC experiment.

## Experimental Section

**Materials.** All Chemicals were obtained from Sigma−Aldrich and used without further purification unless otherwise stated. *N*-Isopropylacrylamide (iPA, 97%) was recrystallized from toluene/hexane (3:2, v/v). *N,N*-ethylmethylacrylamide (EMA) and *N*-*n*-propylacrylamide (nPA) were prepared from the corresponding alkylamines and acryloyl chloride (97%), according to a procedure as reported by Shea et al.[44] A trithiocarbonate (2-dodecylsulfanylthiocarbonylsulfanyl-2-methylpropionic acid, DMP) was prepared according to a previous procedure and used as the RAFT reagent.[45] 2,2′-Azoisobutyronitrile (AIBN, 98%) was recrystallized from methanol. Water was purified with a Millipore Milli-Q system.

The details of the synthesis of the triblock copolymer by 3-step sequential RAFT polymerization have been reported.[41,42] For the synthesis of triblock copolymers (see details in the Supporting Information), a diblock copolymer $PnPA_{124}$-*b*-$PiPA_{80}$ was used as the macro chain transfer agent. EMA (0.483/1.545 g, 4.27/3.67 mmol), $PnPA_{124}$-*b*-$PiPA_{80}$ (2.0/1.6 g, 0.0855/0.0684 mmol), and AIBN (2.81/2.25 mg, 0.0171/0.0137 mmol) were added along with 25 mL of DMSO to 50 mL flasks to synthesize triblock copolymers with different lengths of the PEMA block. (The two sets of numbers are for Tri1 and Tri2, respectively.) After purging with $N_2$ for 20 min, the copolymerization proceeded at 70 °C for 3 h and the products were isolated by dialysis in cellulose dialysis membrane (Spectra/Por 3 purchased from VWR with molecular weight cutoff at 3500) for about 3 days at room temperature and subsequent lyophilization.

The number average molecular weight ($M_n$) and the polydispersity ($M_w/M_n$) of the triblock copolymers were characterized by a combination of gel permeation chromatography (GPC) and $^1$H NMR spectroscopy. GPC measurements were carried out on a Waters 1525 system equipped with a Waters 2410 refractive index detector and Styragel columns (HR3, HR4, and HR6) which provide an effective molecular weight in the range 500 to $10^7$ g mol$^{-1}$. A series of monodisperse polystyrenes (200 to $10^6$ g mol$^{-1}$) were used as the calibration standard. Tetrahydrofuran (THF) was used as the eluent with a flow rate of 1.0 mL min$^{-1}$. The measurement temperature was 35 °C. Data acquisition is performed with Waters Breeze Chromatography Software Version 3.30. $^1$H NMR spectra were recorded on a Bruker-AV400 spectrometer with deuterated chloroform ($CDCl_3$) as the solvent and tetramethylsilane (TMS) as the internal standard.

The trithiocarbonate end group of the polymer from the RAFT process has been removed by thioamidation and then transformed into a thioether by Michael addition with 2-hydroxyethyl acrylate (Supporting Information and Scheme S1).[43] Therefore, the hydrophilic character of the end segment is maintained. Only these terpolymers (Scheme 1) are used in the light scattering experiments.

**Light Scattering (LS).** LS measurements were conducted on an ALV/DLS/SLS-5022F spectrometer with a multi-$\tau$ digital time correlator (ALV5000) and a cylindrical 22 mW Uniphase He−Ne laser ($\lambda_0 = 632.8$ nm) as the light source. In static LS,[46,47] we can obtain the weight-average molar mass ($M_w$) and the z-average root-mean-square radius of gyration ($\langle R_g^2\rangle^{1/2}$ or written as $\langle R_g\rangle$) of scattering objects in a dilute solution or dispersion from the angular dependence of the excess scattering intensity, known as the Rayleigh ratio $R_{vv}(q)$:

$$\frac{KC}{R_{vv}(q)} \approx \frac{1}{M_w}\left(1 + \frac{1}{3}\langle R_g^2\rangle q^2\right) + 2A_2C \qquad (1)$$

**Scheme 1. Chemical Structures of (A) PnPA, (B) PnPA-*b*-PiPA, and (C) PnPA-*b*-PiPA-*b*-PEMA Used in This Study**

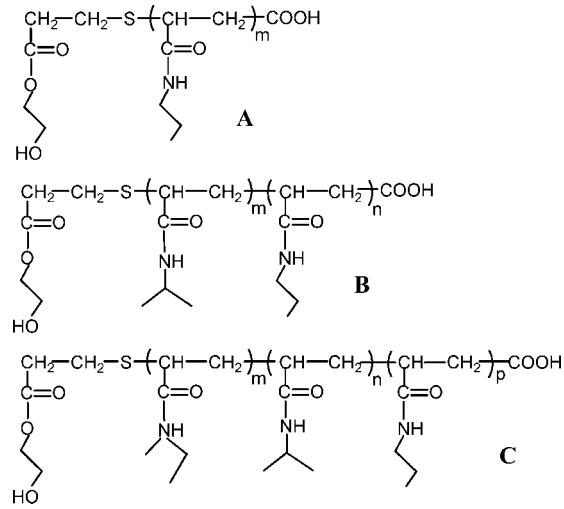


where $K = 4\pi n^2(dn/dC)^2/(N_A\lambda_0^4)$ and $q = (4\pi n/\lambda_0)\sin(\theta/2)$ with $N_A$, $dn/dC$, $n$, and $\lambda_0$ being the Avogadro number, the specific refractive index increment, the solvent refractive index, and the wavelength of the light in a vacuum, respectively, and $A_2$ the second virial coefficient.

In dynamic LS,[48] the Cumulant analysis of the measured intensity−intensity time correlation function $G^{(2)}(q,t)$ in the self-beating mode leads to an average line width ($\langle\Gamma\rangle$) and a line width distribution $G(\Gamma)$. For diffusive relaxation, $\Gamma$ is related to the translational diffusion coefficient ($D$) of the scattering object (polymer chain or colloid particle) in dilute solution or dispersion by $D = (\langle\Gamma\rangle/q^2)_{C\to0,q\to0}$ and further to hydrodynamic radius ($R_h$) from the Stokes−Einstein equation $R_h = k_BT/(6\pi\eta D)$, where $\eta$, $k_B$, and $T$ are the solvent viscosity, the Boltzmann constant, and the absolute temperature, respectively. Dynamic LS measurements were conducted at a small scattering angle ($\theta$) of 15° where the concentration ($C$) was $1 \times 10^{-4}$ g/mL. At such a dilute concentration, the solution is clear at a temperature below ~70 °C. All the solutions were filtered through 0.22-$\mu$m Millipore filters to remove dust and the LS data points were obtained after the measured values were stable. The specific refractive index increment ($dn/dC$) at different temperatures was measured by using a novel differential refractometer.[49]

**Ultrasensitive Differential Scanning Calorimetry (US-DSC).** US-DSC measurements were performed on a VP-DSC calorimeter from MicroCal. The reference cell was filled with deionized water. The copolymer solution with a concentration of $1.0 \times 10^{-3}$ g/mL was degassed at 25 °C for 30 min and equilibrated at 10 °C for 120 min before the heating process. In the cooling process, the solution was equilibrated at 60 °C for 120 min. The scanning rate was 1.0 °C/min. Data analysis including the deconvolution analysis was done by use of the Origin software supplied by the manufacturer. The phase transition temperature ($T_p$) was taken as the central point of the transition. The enthalpy change ($\Delta H$) during the transition was calculated from the integrated area of each peak.

## Results and Discussion

The characteristics of the polymers PnPA, PnPA-*b*-PiPA, and PnPA-*b*-PiPA-*b*-PEMA used (as shown in Scheme 1) are summarized in Table 1. The hydrophilic character of the chain end is maintained by the modification of end group with thioamidation and Michael addition. The hydrophilicity of the parent homopolymers increases in the order of PnPA, PiPA, and PEMA with a phase transition temperature of about 25, 36, and 70 °C, respectively.[42] Previously, we have found that the hydrophilicity of each of the blocks will influence mutually

**Table 1. Conversion, Molecular Weight, and Polydispersity of the Mono-, Di-, and Triblock Copolymers**

| polymer | conversion (%)[a] | $M_n$[b] | $M_w/M_n$[b] |
|---|---|---|---|
| $P(nPA)_{124}$ | 69 | 14 400 | 1.10 |
| $P(nPA_{124}$-*b*-$iPA_{80})$ | 87 | 23 400 | 1.10 |
| $P(nPA_{124}$-*b*-$iPA_{80}$-*b*-$EMA_{44})$ (Tri1) | 85 | 28 400 | 1.14 |
| $P(nPA_{124}$-*b*-$iPA_{80}$-*b*-$EMA_{160})$ (Tri2) | 80 | 41 500 | 1.14 |

[a] Measured by $^1$H NMR. [b] Measured by SEC.

and modify the phase transition temperatures of the individual blocks from those of the corresponding homopolymers.[42] In this work, the temperature-induced phase transition behavior of the triblock copolymers in aqueous solutions is systematically investigated at a microscale with a combination of static and dynamic light scattering techniques.

**Heating Process.** Figure 1A shows the temperature dependence of the hydrodynamic radius $\langle R_h \rangle$ of the stable aggregates formed by the two different copolymers in the heating process. The temperature dependence of $\langle R_h \rangle$ of Tri1 is quite different from that of Tri2. When the temperature increases to 25 °C, corresponding to the LCST of PnPA, $\langle R_h \rangle$ increases abruptly, indicating the aggregation of triblock copolymers. For Tri2 with a longer PEMA block, $\langle R_h \rangle$ decreases slightly in the range of ~32−38 °C due to the collapse of the PiPA chains on the periphery of the micelles. Further increase in temperature to ~53 °C causes a slight decrease in $\langle R_h \rangle$, corresponding to the collapse of the PEMA. The volume phase transition (VPT) temperatures of the blocks are shown in Figure 1A. Finally, Tri2 forms a stable mesoglobule after the three-step phase transition. For Tri1, $\langle R_h \rangle$ continuously increases in the range of ~32−38 °C. Such an increase can be attributed to the aggregation of the micelles. From the results of Tri2, we know that the short PEMA chains on the periphery may have an important effect on the aggregation of the micelles. When the temperature is in the range of 38−45 °C or above ~ 53 °C, $\langle R_h \rangle$ decreases as a result of the collapse of PiPA and PEMA chains and even of the likely further contraction of the collapsed PnPA core.

Figure 1B shows the temperature dependence of the apparent molar mass ($M_w$) of the resultant aggregates in the heating process. Clearly, Tri1 shows a behavior quite different from that of Tri2. At a temperature above 25 °C, the increase in $M_w$

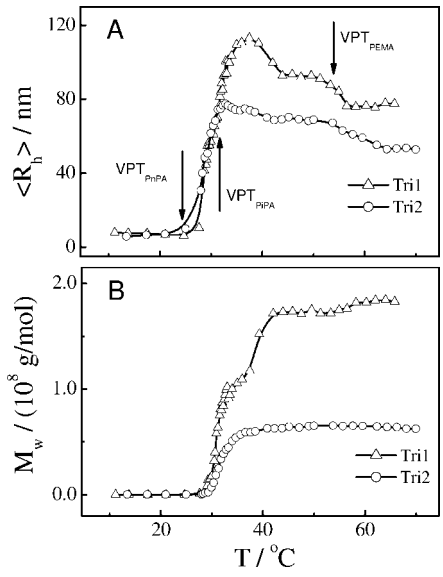


**Figure 1.** Temperature dependence of (A) the hydrodynamic radius $\langle R_h \rangle$ and (B) the apparent molar mass ($M_w$) of the resultant aggregates in the 0.1 mg/mL aqueous solutions of $P(nPA_{124}$-*b*-$iPA_{80}$-*b*-$EMA_{44})$ (Tri1) and $P(nPA_{124}$-*b*-$iPA_{80}$-*b*-$EMA_{160})$ (Tri2) in the heating process.

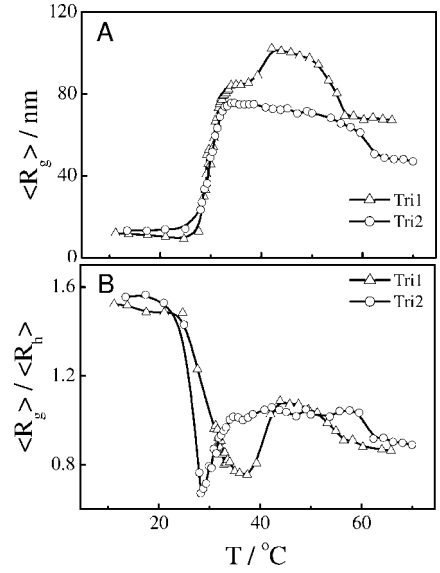


**Figure 2.** Temperature dependence of (A) the radius of gyration $\langle R_g \rangle$ and (B) $\langle R_g \rangle/\langle R_h \rangle$ of the resultant $P(nPA_{124}$-*b*-$iPA_{80}$-*b*-$EMA_{44})$ and $P(nPA_{124}$-*b*-$iPA_{80}$-*b*-$EMA_{160})$ (Tri1 and Tri2) aggregates in the heating process.

indicates the aggregation of both triblock copolymers. For Tri2, $M_w$ varies very little at ~38 °C and above. For Tri1, however, $M_w$ increases quickly again at ca. 38 °C and a plateau can be observed at ca. 45 °C. The second transition suggests the interchain association of different micelles corresponding to the dehydration of the PiPA blocks. Such micellar clusters have been observed in the self-assembly of the block copolymers.[50−53] We have demonstrated that a micellar cluster is easily formed when the chains in the shell of the micelles is not long enough to shield the solvophobic core.[54] In the present case, the PEMA chains on the periphery are too short to shield the hydrophobic core of the micelles when the PiPA chains start to collapse, which makes the clustering of the micelles possible. Note that $\langle R_h \rangle$ in the range of ~38−45 °C decreases while $M_w$ increases. This is due to the competition between the contraction of the PiPA chains and clustering of the micelles. This can be further viewed in terms of $\langle R_g \rangle$ in Figure 2.

Figure 2A shows the temperature dependence of $\langle R_g \rangle$ of the aggregates. At a temperature above 38 °C, $\langle R_g \rangle$ of Tri1 increases, further indicating the clustering of the micelles due to the association of the PiPA chains in different micelles. $\langle R_g \rangle$ drops at ~53 °C, indicating the collapse of PEMA chains on the periphery of the micellar clusters or the micelles.

The temperature dependence of the ratio of the radius of gyration to hydrodynamic radius ($\langle R_g \rangle/\langle R_h \rangle$) is shown in Figure 2B. $\langle R_g \rangle/\langle R_h \rangle$ can describe the structure of a polymer chain or a particle.[55,56] For uniform nondraining spheres, hyperbranched clusters and random coils, the $\langle R_g \rangle/\langle R_h \rangle$ values were found to be ~0.774, 1.0−1.2 and 1.5−1.8, respectively.[56] A spherical micelle generally has a $\langle R_g \rangle/\langle R_h \rangle$ of 0.7−0.8. For Tri1, as temperature increases from 10 to 35 °C, $\langle R_g \rangle/\langle R_h \rangle$ decreases from 1.5 to 0.8, clearly indicating the collapse of the chains and the formation of micelles. $\langle R_g \rangle/\langle R_h \rangle$ increases from 0.8 to 1.0 in the range of 35~45 °C, indicating that the micelles may be forming a cluster. At a temperature above ~53 °C, $\langle R_g \rangle/\langle R_h \rangle$ decreases and finally levels off, indicating that the clusters become dense after the collapse of the PEMA chains on the periphery. Likewise, for Tri2, $\langle R_g \rangle/\langle R_h \rangle$ decreases from ~1.5 to 0.7 in the range of ~10−28 °C, indicating the formation of micelles with PnPA as the core and PiPA and PEMA as the shell. The subsequent increase of $\langle R_g \rangle/\langle R_h \rangle$ starting at ~28 °C can be attributed to the competition between the contraction of the PiPA

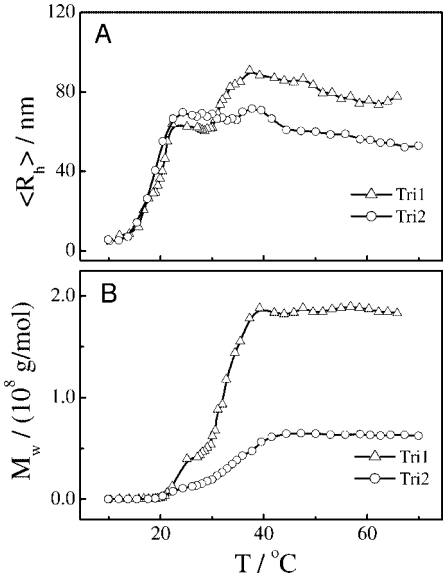


**Figure 3.** Temperature dependence of (A) the hydrodynamic radius $\langle R_h \rangle$ and (B) apparent molar mass ($M_w$) of the resultant P(nPA$_{124}$-*b*-iPA$_{80}$-*b*-EMA$_{44}$) and P(nPA$_{124}$-*b*-iPA$_{80}$-*b*-EMA$_{160}$) (Tri1 and Tri2) aggregates in the cooling process.

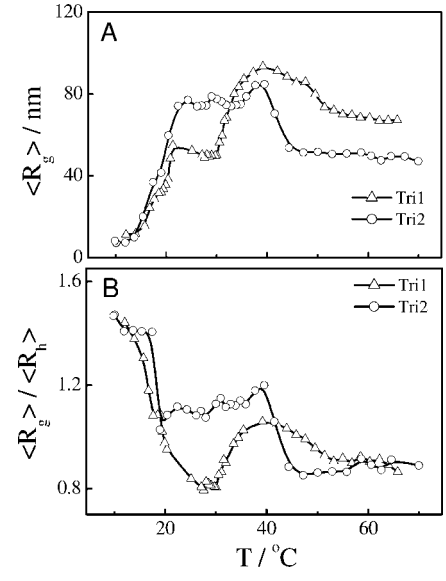


**Figure 4.** Temperature dependence of (A) the radius of gyration $\langle R_g \rangle$ and (B) $\langle R_g \rangle / \langle R_h \rangle$ of the resultant P(nPA$_{124}$-*b*-iPA$_{80}$-*b*-EMA$_{44}$) and P(nPA$_{124}$-*b*-iPA$_{80}$-*b*-EMA$_{160}$) (Tri1 and Tri2) aggregates in the cooling process.

chains and the steric repulsion-induced stretching of PEMA chains.[57] At temperatures above 53 °C, the micelles become denser, so that $\langle R_g \rangle / \langle R_h \rangle$ decreases and levels off.

In short, the PEMA chains in Tri2 are long enough so that the Tri2 micelles exhibit a two-stage collapse in the heating process corresponding to the collapse of the PiPA and PEMA chains, respectively. For Tri1, the shorter PEMA chains on the periphery of the micelles cannot shield the more hydrophobic PnPA and PiPA core completely, so that the PiPA chains in different micelles associate, leading to the formation of micellar clusters.

**Cooling Process.** The dissolution of the aggregates in the cooling process may provide insight to the origin of the micellar clusters. As shown in Figure 3A, $\langle R_h \rangle$ of Tri2 slightly increases in the range of 60∼45 °C and 45∼38 °C, corresponding to the swelling of PEMA and PiPA blocks, respectively. The decrease in $\langle R_h \rangle$ in the range of 38∼24 °C indicates the dissolution of the micelles. $\langle R_h \rangle$ changes little below ∼15 °C, indicating the complete dissolution of the micelles. For Tri1, the change of $\langle R_h \rangle$ is similar to that in the heating process. $\langle R_h \rangle$ increases slightly when the temperature is lowered to ∼53 °C due to the swelling of PEMA chains. When the solution is cooled to 38 °C, $\langle R_h \rangle$ decreases sharply probably due to the disassociation of the micellar clusters. When the temperature is decreased to ∼24 °C, the micelles begin to dissolve, causing the sharp decrease in $\langle R_h \rangle$. Finally, the micelles completely dissolve into copolymer chains at ∼ 15 °C. Note that the complete dissolution temperature (∼15 °C) is lower than the aggregation temperature (∼25 °C) in the heating process (Figure 1). The hysteresis is formed probably due to the formation of additional interchain and intrachain hydrogen bonds in the collapsed state of the PiPA and PnPA chains.[58−60]

The two-stage disintegration of the micellar clusters of Tri1 may also be reflected in the temperature dependence of $M_w$ in Figure 3B. For Tri1, $M_w$ begins to decrease at ∼38 °C because of the dissolution of the micellar clusters. Further cooling of the solution to ∼28 °C leads to a sudden decrease in $M_w$ due to the dissolution of the micelles. When the temperature is decreased to ∼15 °C, $M_w$ becomes much lower and levels off, indicating the complete dissolution of the micelles into individual chains. For Tri2, when temperature decreases from 45 to 15 °C, $M_w$ decreases continuously because of the dissolution of the micelles. In comparison with the results in Figure 1B, a clear hysteresis can be observed from the temperature dependence of $M_w$ in Figure 3B. At the same temperature, the aggregates in the cooling process have a higher molar mass than those in the heating process, further revealing that the hysteresis is due to the formation of interchain and intrachain hydrogen bonds between different chain segments of the collapsed PiPA and PnPA chains in the heating process. It takes more time to disrupt these hydrogen bonds and dissolve the aggregates in the cooling process.[58−60]

Figure 4A shows the temperature dependence of $\langle R_g \rangle$ in the cooling process. For Tri1, the decrease of $\langle R_g \rangle$ in the range of 38∼30 °C also indicates that the micellar clusters are swollen and disassociate into micelles. When the temperature is lowered to ∼10 °C, the small $\langle R_g \rangle$ indicates that the micelles are dissolved completely. For Tri2, $\langle R_g \rangle$ increases in the range of 45∼38 °C, corresponding to the swelling of PEMA. The slight decrease of $\langle R_g \rangle$ in the range of 38∼30 °C is due to the dissolution of the micelles. When temperature is below ∼15 °C, $\langle R_g \rangle$ decreases abruptly due to the complete dissolution of the micelles.

Figure 4B shows the temperature dependence of $\langle R_g \rangle / \langle R_h \rangle$ in the cooling process. For Tri1, $\langle R_g \rangle / \langle R_h \rangle$ increases from 0.9 to 1.0 and decreases to 0.8 when temperature is decreased from 60 to 30 °C, indicating the micelle clusters are swollen and disassociate into micelles. At a temperature below 15 °C, $\langle R_g \rangle / \langle R_h \rangle$ increases from 0.8 to 1.5, indicating that the micelles disassociate into individual chains. For Tri2, $\langle R_g \rangle / \langle R_h \rangle$ increases from 0.8 to 1.2 in the range of 45∼38 °C, corresponding to the swelling of PEMA on the periphery. $\langle R_g \rangle / \langle R_h \rangle$ is ∼1.1 in the range of 38∼20 °C while $M_w$ continuously decreases, indicating the dissociation of the micelles. The increase in $\langle R_g \rangle / \langle R_h \rangle$ from 1.1 to 1.4 at lower temperatures reveals that the micelles disassociate into individual chains completely.

**Microcalorimetry.** We also examined the aggregation by microcalorimetry. Figure 5 shows the effect of the block length of PEMA on the specific heat capacity ($C_p$) of triblock copolymers in one heating−cooling cycle, where the positive and negative $C_p$ values correspond to the endothermic and exothermic processes, respectively. In the heating process, the phase transition temperature ($T_p$) shifts to a higher temperature

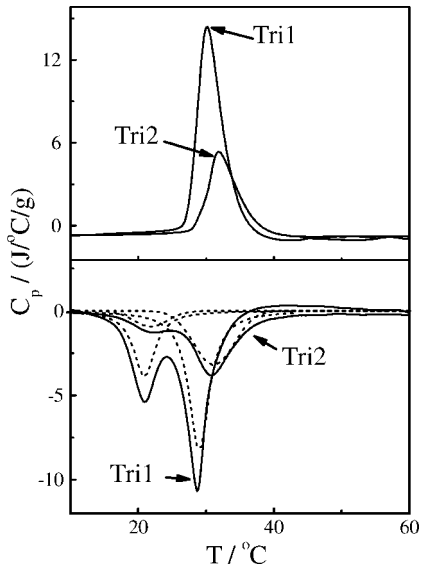


**Figure 5.** Temperature dependence of the specific heat capacity ($C_p$) of triblock copolymers in one heating-and-cooling cycle, where the scanning rate is 1.0 °C/min. The dashed lines show the deconvolution of the peaks for Tri1 and Tri2 in the cooling process.

**Table 2. Thermodynamic Parameters of the Phase Transition of Triblock Copolymers in the Heating and Cooling Processes**

| | heating | | cooling | | | |
|---|---|---|---|---|---|---|
| sample | $T_p$ (°C) | $\Delta H$ (J/g) | $T_{p1}$ (°C) | $\Delta H_1$ (J/g) | $T_{p2}$ (°C) | $\Delta H_2$ (J/g) |
| Tri1 | 30.2 | 68.0 | 20.9 | −28.4 | 28.7 | −56.0 |
| Tri2 | 31.9 | 34.0 | 21.0 | −7.3 | 30.5 | −20.6 |

as the PEMA length increases, since PEMA is more hydrophilic than PnPA and PiPA. The enthalpy change ($\Delta H$) due to the collapse of the PnPA and PiPA chains during the phase transition of Tri1 is much higher than that of Tri2 (Table 2). This is because the PEMA block in Tri1 is shorter than in Tri2, and the fraction of PnPA and PiPA blocks in the former is higher than in the latter. Note that the collapse of PnPA and PiPA blocks cannot be differentiated from each other in the heating process because their VPTs are close to each other and the collapse is quick. However, the exothermic peaks can be deconvoluted into two peaks in the cooling process (Figure 5, dashed lines). The peak located at ∼29.0 °C is attributed to the swelling of PiPA blocks and the dissolution of the aggregates. As discussed above, it usually takes time to disrupt the additional hydrogen bonds formed in the heating process.[58−60] As the temperature decreases, the micelles swell and dissolve gradually PiPA and then PnPA. The hysteresis enlarges the difference in the swelling of the two blocks, so that the peak located at ∼21 °C associated with the swelling of the PnPA blocks can be observed. On the other hand, since the PiPA block is more hydrophilic than the PnPA block, more energy is needed to swell the chains in the cooling process, so that the peak at ∼29 °C has a lower intensity than the one at ∼21 °C. Nevertheless, no endothermic or exothermic peak around ∼53 °C was observed in either heating or cooling process, due to the very small enthalpy change of the PEMA block.

The micellization of the thermosensitive triblock copolymers is schematically illustrated in Scheme 2. The micellization of Tri1 is quite different from that of Tri2 due to the difference in the length of the PEMA block. For Tri1, the formation of micelles starts at ∼25 °C and the formed micelles aggregate further into micellar clusters when the temperature reaches above ∼38 °C. For Tri2, stable micelles are formed at ∼27 °C and the $\langle R_h \rangle$ of the micelles decreases continuously with the

**Scheme 2. Schematic Illustration of the Micellization of Triblock Copolymers[a]**

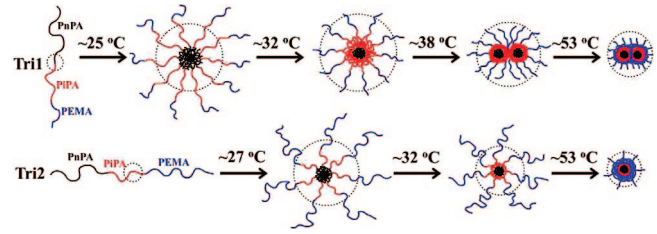


[a] The dash cycles show only the approximate hydrodynamic size.

continuous increase in temperature due to the consecutive collapse of the PiPA and PEMA chains.

## Conclusion

Thermosensitive PnPA-*b*-PiPA-*b*-PEMA triblock terpolymers with different lengths of the final block are shown to form stable micelles. First, the volume phase transition temperature of each of the blocks is influenced by the relative hydrophobicity/hydrophilicity of its neighboring blocks. Second, the micellization process depends on the relative length of the PEMA block. Following the formation of micelles, further increase in temperature leads to the collapse of the PiPA and PEMA chains on the periphery of the micelles. When the PEMA block is short, the PEMA chains cannot shield the hydrophobic PnPA and PiPA core completely, leading to the clustering of the micelles. A longer PEMA block can prevent or delay the formation of micellar clusters. In the cooling process, a hysteresis can be observed due to the formation of additional hydrogen bonds. This finding helps to understand the aggregation of multiblock copolymers in solutions and will help in the design and preparation of useful materials based on the multiple thermosensitivity of this type of polymers.

**Acknowledgment.** Financial support from NSERC of Canada, Canada Research Chair program, National Natural Science Foundation of China (20611120039), and Ministry of Science and Technology of China (2007CB936401) is acknowledged. Y.C. thanks the China Scholarship Council for a scholarship for her stay at University of Montreal.

**Supporting Information Available:** Text giving the synthetic details and the characterization of the triblock copolymers, a scheme showing the preparation of the triblock copolymer, a table of polymer characteristics, and figures showing SEC traces, a $^1$H NMR spectrum, and UV spectra. This material is available free of charge via the Internet at http://pubs.acs.org.

## References and Notes

(1) Gutowska, A.; Bae, Y. H.; Jacobs, H.; Feijen, J.; Kim, S. W. *Macromolecules* **1994**, *27*, 4167–4175.
(2) Zintchenko, A.; Ogris, M.; Wagner, E. *Bioconjugate Chem.* **2006**, *17*, 766–772.
(3) Liang, D. H.; Zhou, S. Q.; Song, L. G.; Zaitsev, V. S.; Chu, B. *Macromolecules* **1999**, *32*, 6326–6332.
(4) Inomata, H.; Goto, S.; Saito, S. *Macromolecules* **1990**, *23*, 4887–4888.
(5) Gehrke, S. H. *Adv. Polym. Sci.* **1993**, *110*, 81–144.
(6) Osada, Y.; Gong, J. P. *Adv. Mater.* **1998**, *10*, 827–837.
(7) Platé, N. A.; Lebedeva, T. L.; Valuev, L. I. *Polym. J.* **1999**, *31*, 21–27.
(8) Liu, H. Y.; Zhu, X. X. *Polymer* **1999**, *40*, 6985–6990.
(9) Xue, W.; Huglin, M. B.; Jones, T. G. J. *Macromol. Chem. Phys.* **2003**, *204*, 1956–1965.
(10) Zhu, X. X.; Avoce, D.; Liu, H. Y.; Benrebouh, A. *Macromol. Symp.* **2004**, *207*, 187–191.

(11) Schilli, C. M.; Zhang, M.; Rizzardo, E.; Thang, S. H.; Chong, Y. K.; Edwards, K.; Karlsson, G.; Mueller, A. H. E. *Macromolecules* **2004**, *37*, 7861–7866.
(12) Bussels, R.; Bergman-Gottgens, C.; Meuldijk, J.; Koning, C. *Polymer* **2005**, *46*, 8546–8554.
(13) Luo, S.; Xu, J.; Zhu, Z.; Wu, C.; Liu, S. *J. Phys. Chem. B* **2006**, *110*, 9132–9139.
(14) Gil, E. S.; Hudson, S. A. *Prog. Polym. Sci.* **2004**, *29*, 1173–1222.
(15) Rodriguez-Hernandez, J.; Checot, F.; Gnanou, Y.; Lecommandoux, S. *Prog. Polym. Sci.* **2005**, *30*, 691–724.
(16) Dimitrov, I.; Trzebicka, B.; Muller, A. H. E.; Dworak, A.; Tsvetanov, C. B. *Prog. Polym. Sci.* **2007**, *32*, 1275–1343.
(17) Aoshima, S.; Kanaoka, S. *Adv. Polym. Sci.* **2008**, *210*, 169–208.
(18) Topp, M. D. C.; Dijkstra, P. J.; Talsma, H.; Feijen, J. *Macromolecules* **1997**, *30*, 8518–8520.
(19) Zhu, P. W.; Napper, D. H. *Macromolecules* **1999**, *32*, 2068–2070.
(20) Gohy, J. F.; Varshney, S. K.; Jerome, R. *Macromolecules* **2001**, *34*, 3361–3366.
(21) Virtanen, J.; Holappa, S.; Lemmetyinen, H.; Tenhu, H. *Macromolecules* **2002**, *35*, 4763–4769.
(22) Nuopponen, M.; Ojala, J.; Tenhu, H. *Polymer* **2004**, *45*, 3643–3650.
(23) Zhang, W. Q.; Shi, L. Q.; Wu, K.; An, Y. G. *Macromolecules* **2005**, *38*, 5743–5747.
(24) Forder, C.; Patrickios, C. S.; Armes, S. P.; Billingham, N. C. *Macromolecules* **1996**, *29*, 8160–8169.
(25) Mertoglu, M.; Garnier, S.; Laschewsky, A.; Skrabania, K.; Storsberg, J. *Polymer* **2005**, *46*, 7726–7740.
(26) Sugihara, S.; Kanaoka, S.; Aoshima, S. *Macromolecules* **2005**, *38*, 1919–1927.
(27) Okabe, S.; Seno, K.; Kanaoka, S.; Aoshima, S.; Shibayama, M. *Macromolecules* **2006**, *39*, 1592–1597.
(28) Hua, F. J.; Jiang, X. G.; Zhao, B. *Macromolecules* **2006**, *39*, 3476–3479.
(29) Dimitrov, P.; Rangelov, S.; Dworak, A.; Tsvetanov, C. B. *Macromolecules* **2004**, *37*, 1000–1008.
(30) Hasan, E.; Zhang, M.; Muller, A. H. E.; Tsvetanov, C. B. *J. Macromol. Sci.—Pure Appl. Chem.* **2004**, *A41*, 467–486.
(31) Sugihara, S.; Kanaoka, S.; Aoshima, S. *J. Polym. Sci. Part A: Polym. Chem.* **2004**, *42*, 2601–2611.
(32) Li, C. M.; Tang, Y. Q.; Armes, S. P.; Morris, C. J.; Rose, S. F.; Lloyd, A. W.; Lewis, A. L. *Biomacromolecules* **2005**, *6*, 994–999.
(33) Li, C. M.; Buurma, N. J.; Haq, I.; Turner, C.; Armes, S. P.; Castelletto, V.; Hamley, I. W.; Lewis, A. L. *Langmuir* **2005**, *21*, 11026–11033.
(34) Madsen, J.; Armes, S. P.; Lewis, A. L. *Macromolecules* **2006**, *39*, 7455–7457.
(35) Sammon, C.; Li, C.; Armes, S. P.; Lewis, A. L. *Polymer* **2006**, *47*, 6123–6130.
(36) Munoz-Bonilla, A.; Fernandez-Garcia, M.; Haddleton, D. M. *Soft Matter* **2007**, *3*, 725–731.
(37) Skrabania, K.; Kristen, J.; Laschewsky, A.; Akdemir, O.; Hoth, A.; Lutz, J. F. *Langmuir* **2007**, *23*, 84–93.
(38) Zhao, X. L.; Liu, W. G.; Chen, D. Y.; Lin, X. Z.; Lu, W. W. *Macromol. Chem. Phys.* **2007**, *208*, 1773–1781.
(39) Skrabania, K.; Li, W.; Laschewsky, A. *Macromol. Chem. Phys.* **2008**, *209*, 1389–1403.
(40) Xu, J.; Luo, S. Z.; Shi, W. F.; Liu, S. Y. *Langmuir* **2006**, *22*, 989–997.
(41) Cao, Y.; Zhu, X. X. *Can. J. Chem.* **2007**, *85*, 407–411.
(42) Cao, Y.; Zhu, X. X.; Luo, J. T.; Liu, H. Y. *Macromolecules* **2007**, *40*, 6481–6488.
(43) Cao, Y.; Zhao, N.; Wu, K.; Zhu, X. X. *Langmuir* **2009**, *25*, 1699–1704.
(44) Shea, K. J.; Stoddard, G. J.; Shavelle, D. M.; Wakui, F.; Choate, R. M. *Macromolecules* **1990**, *23*, 4497–4507.
(45) Lai, J. T.; Filla, D.; Shea, R. *Macromolecules* **2002**, *35*, 6754–6756.
(46) Zimm, B. H. *J. Chem. Phys.* **1948**, *16*, 1099–1116.
(47) Chu, B. *Laser Light Scattering*, 2nd ed.; Academic Press: New York, 1991.
(48) Beme, B. P., R. *Dynamic Light Scattering*; Plenum Press: New York, 1976.
(49) Wu, C.; Xia, K. Q. *Rev. Sci. Instrum.* **1994**, *65*, 587–590.
(50) Xu, R. L.; Winnik, M. A.; Hallett, F. R.; Riess, G.; Croucher, M. D. *Macromolecules* **1991**, *24*, 87–93.
(51) Lombardo, D.; Micali, N.; Villari, V.; Kiselev, M. A. *Phys. Rev. E* **2004**, *70*, 021402.
(52) Pispas, S.; Hadjichristidis, N. *Langmuir* **2003**, *19*, 48–54.
(53) Pispas, S.; Hadjichristidis, N. *Macromolecules* **2003**, *36*, 8732–8737.
(54) Xie, D.; Bai, W.; Xu, K.; Bai, R.; Zhang, G. Z. *J. Phys. Chem. B* **2007**, *111*, 8034–8037.
(55) Burchard, W. *Light Scattering Principles and Development*; Brown, W., Ed.; Clarendon Press: Oxford, U.K., 1996; p 439.
(56) Douglas, J. F.; Roovers, J.; Freed, K. F. *Macromolecules* **1990**, *23*, 4168–4180.
(57) Tu, Y. F.; Wan, X. H.; Zhang, D.; Zhou, Q. F.; Wu, C. *J. Am. Chem. Soc.* **2000**, *122*, 10201–10205.
(58) Ding, Y. W.; Ye, X. D.; Zhang, G. Z. *Macromolecules* **2005**, *38*, 904–908.
(59) Cheng, H.; Shen, L.; Wu, C. *Macromolecules* **2006**, *39*, 2325–2329.
(60) Wu, C.; Wang, X. H. *Phys. Rev. Lett.* **1998**, *80*, 4092–4094.

MA802801H